Available online at www.sciencedirect.com
SCIENCE DIRECT®
Surface Science 544 (2003) 285–294
SURFACE SCIENCE
www.elsevier.com/locate/susc

Adsorption and thermal dissociation of pyrrole on Si(1 0 0)-2×1

Ming-Hua Qiao [a,b], Feng Tao [a], Yong Cao [a,b], Guo-Qin Xu [a,*]

[a] *Department of Chemistry, National University of Singapore, 10 Kent Ridge Crescent, Singapore 119260, Singapore*
[b] *Department of Chemistry, Fudan University, Shanghai 200433, PR China*

Received 27 May 2003; accepted for publication 25 August 2003

Abstract

The adsorption and thermal reaction of pyrrole on Si(1 0 0)-2×1 have been studied using X-ray and ultra-violet photoelectron spectroscopies (XPS and UPS) and high resolution electron energy loss spectroscopy (HREELS). At low exposures, Pyrrole chemisorbs molecularly at 120 K with its ring parallel to the surface via the π-interaction. The increase in coverage causes tilting of chemisorbed molecules towards the surface normal, attributable to the adsorbate–adsorbate interactions. At ~350 K, the N–H bond scission of the π-bonded species occurs, resulting in Si–H and vertically N-bonded pyrrolyl on the surface. The pyrrolyl species is thermally stable to 700 K. Compared to furan or thiophene on Si(1 0 0), this higher thermal stability is ascribed to the passivation effect of the H-atoms from N–H bond dissociation and the less strain within the pyrrolyl–substrate complex. Further annealing to 900 K results in the formation of silicon carbide and silicon nitride on the substrate.

Keywords: Electron energy loss spectroscopy (EELS); Visible and ultraviolet photoelectron spectroscopy; X-ray photoelectron spectroscopy; Chemisorption; Surface chemical reaction; Silicon; Aromatics

1. Introduction

The organic functionalization or modification of Si(1 0 0) is of great technological importance for developing new Si-based microelectronics [1]. Previous investigations in this area mainly involve the binding of some simple unsaturated hydrocarbons [2–4], and six-membered aromatics (benzene [5] and its derivatives including toluene [6,7], xylene [7], styrene [8] and phenyl isothiocyanate [9]).

Five-membered heteroatom cyclic aromatics including furan, thiophene and pyrrole are another kind of practically interesting and valuable functional organic molecules [10–13]. Recent experimental and theoretical studies on the interaction of furan and thiophene with Si(1 0 0) clearly demonstrated a [4 + 2] cycloaddition mechanism between their α-C atoms and a silicon surface dimer, forming 2,5-dihydrofuran- and 2,5-dihydrothiophene-like intermediates, respectively [14–16]. In this bonding configuration, furan or thiophene functions as a "diene" and the silicon surface dimer as a "dienophile", leading to a Si_2C_4 ring-like

* Corresponding author. Tel.: +65-6874-3595; fax: +65-6779-1691.
E-mail address: chmxugq@nus.edu.sg (G.-Q. Xu).

0039-6028/$ - see front matter © 2003 Elsevier B.V. All rights reserved.
doi:10.1016/j.susc.2003.08.039

structure. However, for pyrrole, the situation is slightly more complicated. In addition to the possible [2 + 2] or [4 + 2] cycloaddition reaction through its C=C bonds, the dissociative adsorption through the breakage of N–H bond to form H-atom and pyrrolyl binding on Si(1 0 0) is another possibility, preserving the ring aromaticity in the resulting reaction products. Thus, understanding the selectivity in the binding of pyrrole on Si(1 0 0) is scientifically interesting and significant. We briefly reported the dissociative adsorption of pyrrole on Si(1 0 0)-2×1 at room temperature through the breakage of its N–H bond, forming adsorbed pyrrolyl and H-atoms [17]. In addition, the possible concurrent occurrence of α-C–H dissociation was also suggested [18]. Theoretical studies carried out to provide insights into the reaction mechanism of pyrrole on Si(1 0 0)-2×1 show that dissociative reactions, leading to the partial fragmentation of the molecule, is energetically most favored for pyrrole chemisorbed on Si(1 0 0) [19]. However, the detailed knowledge on the binding configuration of pyrrole on Si(1 0 0)-2×1 as a function of surface temperature is still to be gained. In particular, at low-temperatures pyrrole possibly displays distinctly different chemisorption behavior compared to the dissociative adsorption observed at room temperature. Furthermore, the thermal decomposition of pyrrole on silicon is important in its own right, as SiC is a material for high-temperature, high-power and high-frequency applications in microelectronics and electro-optical devices [20–22] and Si_3N_4 is a potential high-temperature and high-strength structural material [23]. All these motivate the present systematic investigation on the adsorption and thermal reaction of pyrrole on Si(1 0 0)-2×1 using combined XPS, UPS and HREELS techniques.

2. Experimental

The experiments were performed in two UHV chambers both with a base pressure lower than 2×10^{-10} Torr. One of them is equipped with a high resolution electron energy loss spectrometer (HREELS, LK-2000-14R). HREELS measurements were taken in a specular geometry. The electron beam with energy of 5.0 eV impinges on the surface at an incident angle of 60° with respect to the surface normal. A typical instrumental resolution of 60 cm^{-1} was achieved. Photoelectron studies were carried out on the other chamber mainly equipped with an X-ray source, a He discharge lamp and a concentric hemispherical energy analyzer (CLAM2, VG). XPS spectra were acquired using Al Kα radiation ($h\nu = 1486.6$ eV) and 20 eV pass energy. For XPS the binding energy (BE) scale is referenced to the peak maximum of Si 2p line (BE = 99.3 eV) of a clean Si(1 0 0) [24] with a full width at half maximum (FWHM) of less than 1.2 eV. The valence band spectra were excited by He II ($h\nu = 40.8$ eV) radiation due to its wider energy window and referenced to the Fermi level (E_F) of the metallic tantalum sample holder. In this case the pass energy was 10 eV.

The Si(1 0 0) samples were cut from p-type boron-doped silicon wafers (99.999%, 1–30 Ω cm, Goodfellow) and mounted as follows. Two pieces of Si(1 0 0) single crystal with a same dimension ($18\times10\times0.38$ mm^3) were first covered by evaporation with a thin Ta layer on the unpolished back for homogeneous heating and cooling. A piece of Ta foil (0.025 mm thick, Goodfellow) was sandwiched between the two so-treated silicon samples as heater. They were clamped using two Ta clips for fixation. The in-between Ta foil was then spot-welded to Ta rods at the bottom of the manipulator. A 0.003 in. W–5%Re/W–26%Re thermocouple was attached to the center of one silicon sample using ultra-high temperature ceramic adhesive (Aremco 516) for temperature measurement and control. Such mounted silicon sample can be resistively heated to 1400 K and conductively cooled to 120 K by liquid nitrogen. The temperature distribution on the sample was within ±10 K at 1000 K as identified by an IR pyrometer.

The silicon sample was then thoroughly degassed at 900 K overnight under ultra-high vacuum. Surface contaminants, such as carbon and oxygen were removed by repeated Ar^+ bombardment and annealing to 1300 K. Surface cleanliness was confirmed by XPS, UPS and HREELS. Pyrrole (98%, Aldrich) was purified by freeze–pump–thaw cycles prior to use. Dosing was accomplished

by backfilling the chamber through a variable leak valve. The exposures were calculated based on the dosing pressure and time without ion gauge sensitivity calibration.

3. Results

3.1. Adsorption at 120 K

X-ray photoelectron spectroscopy measurements were employed to investigate the chemical states of adsorbed pyrrole on Si(1 0 0)-2×1. The C 1s and N 1s spectra of pyrrole following a sequence of exposures at 120 K are shown in Fig. 1a and b, respectively. The corresponding peak areas are fitted and plotted in Fig. 2. Below 1.0 L exposure (1 L = 1×10^{-6} Torr s), the N 1s peak at 399.1 eV grows up preferentially. At higher exposures, the high binding energy peak at 400.3 eV becomes dominant with gradual attenuation of the low binding energy feature. In contrast, for C 1s there is only a single sharp peak at 284.7 eV within the whole exposures. For gaseous pyrrole, the core level binding energies relative to the vacuum level are at 289.8, 290.8 and 406.1 eV for α-, β-C 1s and N 1s, respectively [25]. Due to the solid state broadening effect, only the convolution of the C 1s peaks was observed in the present case. Taking the average of the binding energies of the C 1s photoelectron peaks of gaseous pyrrole, the binding energy difference between N 1s and C 1s (115.8 eV) is then in excellent agreement with that of pyrrole at high exposure on Si(1 0 0)-2×1 (115.6 eV). Thus the 284.7 and 400.3 eV peaks are attributed to photoemissions from C 1s and N 1s core-levels of physisorbed pyrrole, supposing that the local electrostatic potential and the relaxation energy are the same for the ring atoms. Their growth behavior at high exposures is in agreement with the physisorption character. It should be noted that the C 1s/N 1s intensity ratio remains almost constant even at low pyrrole exposures.

The physisorption character of pyrrole on Si(1 0 0)-2×1 at high exposures and 120 K is further confirmed by He II UPS spectra, as shown in

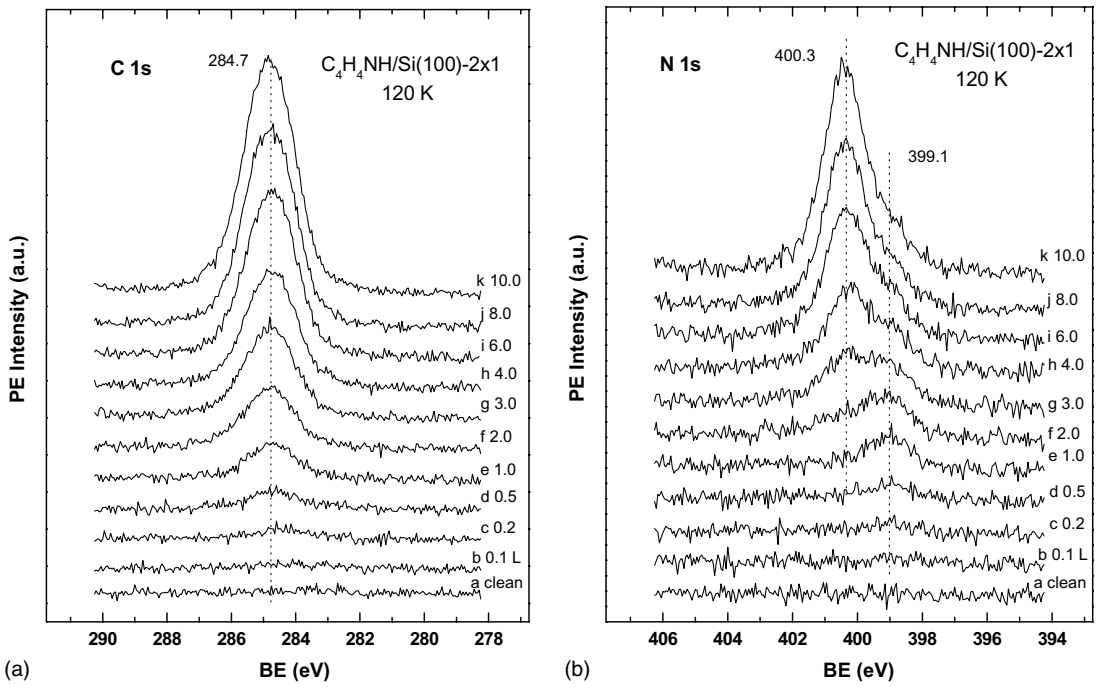

Fig. 1. (a) C 1s and (b) N 1s XPS spectra of pyrrole on Si(1 0 0)-2×1 as a function of pyrrole exposures at 120 K. $h\nu = 1486.6$ eV, pass energy = 20 eV.

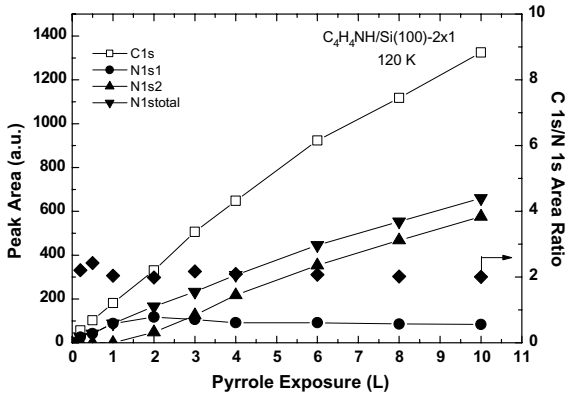

Fig. 2. Plot of individual and total C 1s and N 1s XPS peak intensities versus pyrrole exposures at 120 K.

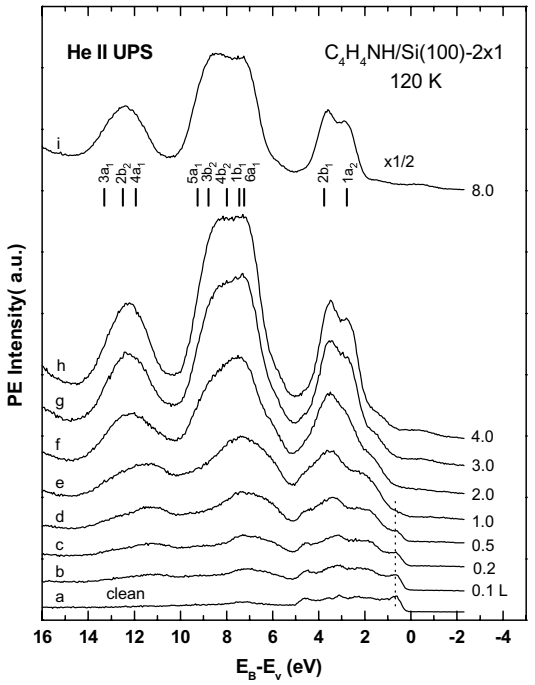

Fig. 3. Coverage-dependent He II ($h\nu = 40.8$ eV) UPS spectra for pyrrole on Si(1 0 0)-2×1 at 120 K. The bar graph at the bottom of (i) indicates the gas phase ionization potentials of pyrrole [19], which are shifted to align with the multilayer spectrum. Pass energy = 10 eV.

Fig. 3. When the Si(1 0 0)-2×1 surface was exposed to 8.0 L of pyrrole at 120 K, peaks at 2.88, 3.61, 12.35 eV and a broad feature ranging from 5 to 10 eV below E_F are noted in Fig. 3i. The energy separations among these peaks compare favorably with those for the gaseous pyrrole valence band spectrum [26], shown here in the form of bar graph obtained by considering work function and the relaxation effect. The good agreement between the UPS results for gaseous pyrrole and pyrrole adsorbed on Si(1 0 0) allows us to assign the first two bands at 2.88 and 3.61 eV to be of π character mainly localized on α- and β-carbons, respectively. The following features are owing to C–C, N nonbonding lone pair, C–N, and C–H σ-orbitals.

At low pyrrole exposures the valence band features are quite similar to those of the condensed pyrrole overall, which implies that no strong perturbation of the ring structure occurred upon chemisorption. However, the surface state at ~0.7 eV below E_F, the bonding "dangling bond" (π_b) level of the silicon surface dimer [27], is completely quenched above 1.0 L dosage, correlating well with the saturation of the chemisorbed pyrrole revealed by XPS. The loss of the surface state strongly suggests its participation in the surface reaction.

Adsorption of pyrrole on Si(1 0 0)-2×1 was further studied by HREELS. Fig. 4a is the vibrational spectrum for 0.5 L pyrrole exposure at 120 K. It is interesting to note that there are only loss peaks at 379, 608 and 739 cm^{-1}, while features above 739 cm^{-1} are essentially unavailable. In addition we did not observe any hydrogen splitting from pyrrole molecule upon adsorption, as this would lead to a distinct Si–H stretching peak at ~2100 cm^{-1} accordingly [28]. At 1.5 L exposure, the HREELS signals are weak, which suggests a random packing of the adsorbates on the surface. Nevertheless, the main molecular vibrational features of pyrrole can be identified in the HREELS spectrum. At higher exposures, the loss features at 583, 752, 872, 1063, 1137, 1364, 1460, 1531, 3126 and 3390 cm^{-1} become well defined. Their assignments are given in Table 1 by comparing with the infrared analysis of vapor phase pyrrole [29] and the HREELS result for pyrrole on Cu(1 0 0) at 170 K [30]. In brief, the 583 and 752 cm^{-1} peaks are attributable to the γ(ring) and γ(CH) modes of B_2 symmetry for intact pyrrole, with the in-plane modes of A_1 and B_1 symmetries ranging from 1063 to 3400 cm^{-1}. For the vibrational region of 1200–

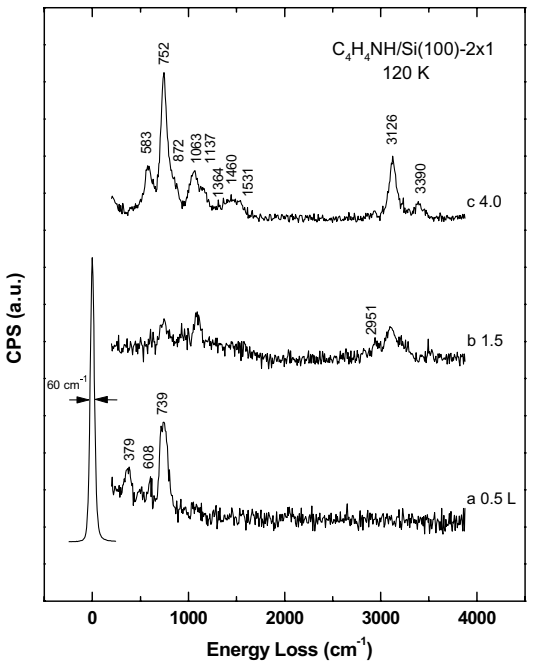

Fig. 4. HREELS spectra of pyrrole on Si(1 0 0)-2×1 at 120 K. $E_p = 5.0$ eV, specular mode.

Table 1
Assignment of the vibrational frequencies for pyrrole adsorbed on Si(1 0 0)-2×1 at 120 K (unit in cm^{-1})

Gas phase[a]	Cu(1 0 0) multilayer[b]	Si(1 0 0)-2×1 multilayer (this work)	Assignment[a]
565	600	583	γ(NH)(B_2)
768	760	752	γ(CH)(B_2)
869	880	872	δ(ring)(B_1)
1047			δ(CH)(A_1)
	1050	1063	
1076			δ(CH)(B_1)
1146	1160	1137	δ(NH)(B_1)
1290			
1380		1364	
	1310		ν(ring)(A_1)
1418		1460	
	1500		ν(ring)(B_1)
1466		1531	
1531			
3133	3120	3126	ν(CH)(A_1)
3400	3380	3390	ν(NH)(A_1)

[a] Ref. [35].
[b] Ref. [36].

1600 cm^{-1}, there are six peaks associated with the ring vibrations in the infrared spectrum of gaseous molecules. However, due to the limited resolution of HREELS spectrometer and the possible effects of condensed phase, only three peaks in this region are reluctantly resolved, similarly observed for physisorbed pyrrole on Cu(1 0 0) at low temperature [36]. Therefore, Table 1 shows that physisorbed multilayer is formed at exposure higher than 4.0 L and the low temperature of 120 K, consistent with the XPS and UPS results which imply the formation of physisorbed layer at high exposures.

3.2. Thermal evolution and conversion of bonding modes

When a 10.0 L pyrrole exposed surface at 120 K was annealed to 150 K, both C 1s and N 1s peak intensities were attenuated accordingly, while the physisorbed features were still dominant, as illustrated in Fig. 5. At 200 K, a reduction of signal intensity by ~70% for both C 1s and N 1s was noted, indicating a substantial desorption of physisorbed pyrrole. The C 1s and N 1s peaks, now dominant at 284.7 and 399.1 eV respectively, are identical with those of the chemisorbed pyrrole below 2.0 L exposure at 120 K. From 200 to 300 K, the N 1s peak maximum remained constant, while the C 1s peak shifts gradually from 284.7 to 284.5 eV. It is worth to note the sudden decrement of the C 1s binding energy by 0.3 eV from 300 to 350 K, which strongly suggests the change of the chemical environment of the adsorbate. On the other hand, no discernable binding energy shift was observed for N 1s at the same temperature, which will be discussed and detailed in following. From 350 to 600 K, the C 1s and N 1s spectra are essentially unchanged in both peak intensity and binding energy, showing the high thermal stability of the resulting surface species. Only annealing to 780 K leads to a loss of these peaks with a small N 1s feature emerging at ~397.3 eV, indicative of the formation of some silicon nitride [31,32]. Meanwhile, the C 1s peak only shifted by 0.1 eV to lower binding energy. At 900 K, the carbonaceous moiety thoroughly decomposed to form silicon carbide with C 1s binding energy of 282.9 eV [33].

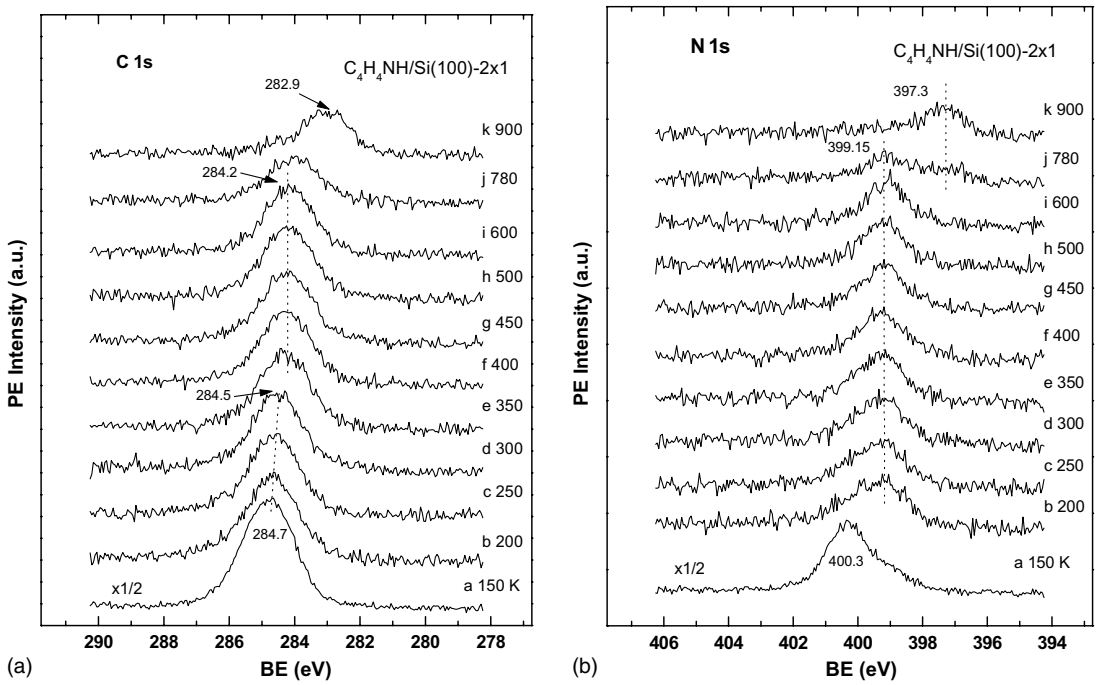

Fig. 5. (a) C 1s and (b) N 1s spectra obtained after annealing the Si(1 0 0) sample pre-exposed with 10.0 L pyrrole at 120 K to various temperatures. $h\nu = 1486.6$ eV, pass energy = 20 eV.

A simple calculation shows that about 50% of carbon and nitrogen are left on the surface relative to the coverage of pyrrole-related species at 350 K which was verified to be the N-bonded pyrrolyl by HREELS shown below.

The thermal effect on the HREELS spectra of 2.0 L pyrrole-dosed Si(1 0 0) is illustrated in Fig. 6. As the sample was warmed to 200 K, loss peaks at 733 and 1089 cm^{-1} are developed from the diffuse feature at 120 K. The small feature at about 3400 cm^{-1}, characteristic of the ν(NH) vibrational mode [29], still exists. However, further annealing to 350 K led to dramatic change in the vibrational spectrum as compared to that at 200 K. It is also quite different from that of the 0.5 L pyrrole-dosed surface at 120 K (Fig. 4). Firstly, the absolute reflectivity of the surface was considerably enhanced, meaning the ordering of the adsorbate on the silicon substrate. Secondly, the decrease in intensity of the ν(NH) mode at $\sim$3400 cm^{-1}, the emergence of the ν(SiH) mode at $\sim$2100 cm^{-1} and the preservation of other pyrrole-related modes clearly demonstrate that at 350 K pyrrole chemisorbs on Si(1 0 0)-2×1 through deprotonation of the N–H group and the formation of a Si–N linkage between the substrate and the pyrrolyl ring. Meanwhile, the hydrogen atom from the breakage of N–H bond saturates the neighboring Si dangling bond to form Si–H bond. A similar surface reaction process has been suggested for aniline [34,35] and 1,4-phenylenediamine [36] on Si(1 0 0). In Fig. 6c, the peaks at 726, 811, 1450 and 1556 cm^{-1} are attributed to ring stretching/deformation modes and C–H out-of-plane bending mode, respectively. The loss features at 1067 and 1187 cm^{-1} can be assigned to C–H in-plane bending modes. The significant increase of intensity of C–H in-plane bending modes (Curves c–e in Fig. 6), compared to those for molecularly chemisorbed pyrrole at a temperature lower than 350 K (Curve b in Fig. 6), strongly suggests that the chemisorbed pyrrolyl ring stands almost upright on Si(1 0 0) at the temperature between $\sim$350 and $\sim$700 K as shown in Scheme 1. The loss features at

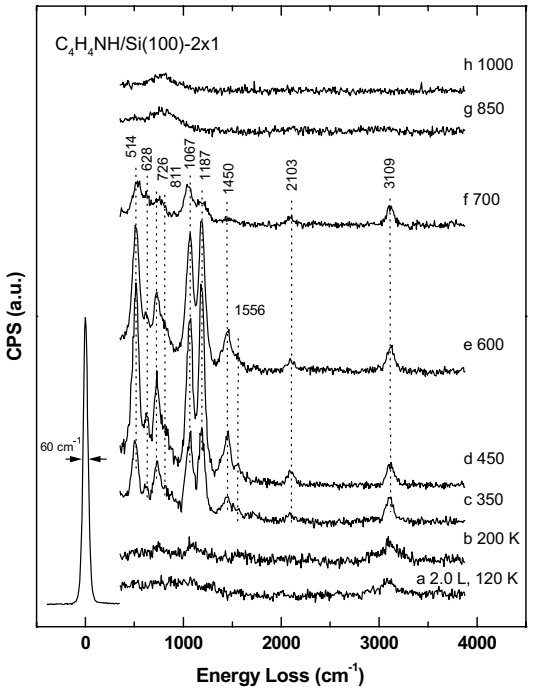

Fig. 6. HREELS spectra after 2.0 L pyrrole exposure at 120 K and annealing the sample to various temperatures. $E_p = 5.0$ eV, specular mode.

628 and 3109 cm^{-1} are assigned to Si–H bending mode and the C–H stretching mode, while the loss feature at 514 cm^{-1} is attributable to Si–N stretching vibration [36,37]. By fitting the C 1s spectrum at 350 K and using room temperature saturated benzene layer on Si(1 0 0) as a reference [38], we estimated the saturation coverage of ~0.47 for pyrrolyl with respect to the surface atomic density of Si(1 0 0)-2×1 (6.78×10^{14} cm^{-2}). It is expected that the remaining silicon surface atoms were covered with hydrogen atoms.

The ordering of the surface assembly continued at 450 K, while at 600 K an attenuation of all vibrational features occurs, reflecting the partial desorption and/or dissociation of the surface species. It is noticeable that further annealing to 700 K results in substantial attenuation of the vibrational features of pyrrolyl, but the main features indicate that the characteristic aromatic ring structure is still retained, which exhibits the remarkable thermal stability of the pyrrolyl assembly on Si(1 0 0)-2×1. Subsequent annealing to 850 K or above leads to the formation of broad features around 800 cm^{-1} associated with Si-carbide or Si-nitride species [32,33,39] due to the complete decomposition of the Si–N linked pyrrolyl ring on the silicon surface.

4. Discussion

Pyrrole, like benzene, is a planar aromatic molecule with six π-electrons. However, as there are only five ring atoms of pyrrole, its electron density is higher than that of benzene and thus the molecule is classified as "π-electron excessive" aromatic molecule [40]. On the other hand, the existence of heteroatom inevitably leads to inhomogeneous electron distribution within the whole ring system. Moreover, pyrrole is a weak acid due to the N–H group, of about the same strength as simple alcohols; its pK_a in aqueous solution is 17.5 [40]. Therefore, more bonding

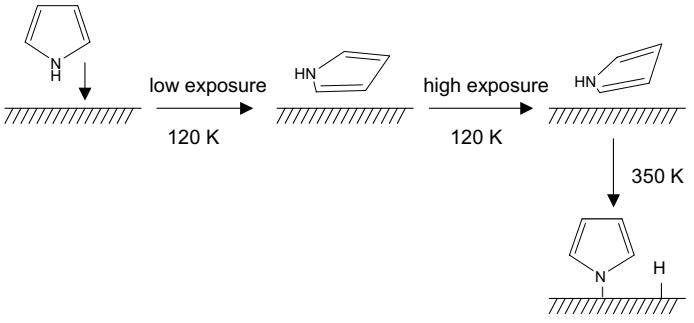

Scheme 1. Bonding configurations for pyrrole on Si(1 0 0)-2×1.

configurations compared to benzene are expected for pyrrole. Actually, for thiophene and furan, its sulfur and oxygen analogues, bonding through the ring π-electrons or the α-carbon [30,41–44] has been observed on single crystal metal surfaces, which can be attributed to their ring π system or a higher electron density on α -carbons than that on β-carbons [40]. In recent studies, the conjugate addition of thiophene or furan with Si(1 0 0)-2×1 has also been verified, in which thiophene or furan functions as diene and silicon surface dimer as dienophile, forming the C_4Si_2 ring structure [14,15].

However, for pyrrole on metal single crystals except for the parallel π-bonded [30,45–48] and the tilt N-bonded configurations after N–H bond scission [46,48,49], no substitution at carbon has ever been observed. In the present study, when the pyrrole-dosed surface was annealed to 350 K, HREELS unambiguously reveals the formation of vertical N-bonded pyrrolyl species on the surface. From the kinetic viewpoint, electrophilic substitution at the α position should be highly favorable since it will lead to more than one resonance structures which may appreciably stabilize the transition state [40]. On the other hand, photodissociation of pyrrole at both 193 and 248 nm has recently provided bond dissociation energies (BDEs) of 88 ± 2 and 112.5 ± 2 kcal mol^{-1} for the N–H and C–H bonds via photofragment translational spectroscopy [50]. And the B3LYP/6-31G(d) calculation nicely verified the above observation (BDEs for α-C–H, β-C–H and N–H are 117.6, 118.1 and 89.8 kcal mol^{-1}, respectively) [51]. If the breakage of α-C–H occurs, the Si–C stretching mode should appear at around 400–800 cm^{-1} ; but HREELS spectra do not present such a peak which can be assigned to ν(SiC). However, the possible overlapping of the Si–C vibrational peak with the vibrational modes of pyrrolyl species or Si–H bending mode in this region can not be ruled out. Combined with the dissociation energies of α-C–H and N–H from experiment [50] and theoretical calculation [51], it seems reasonable to conclude that the dissociative reaction of pyrrole on Si(1 0 0) follows mainly a thermodynamically controlled pathway rather than the kinetically controlled one.

As compared to the surface intermediate at 350 K, the ascription of the low-exposure low-temperature species is not so straightforward. At exposures below 1.0 L at 120 K, a chemisorbed state can be identified, which is characterized by the C 1s and N 1s peaks at 284.7 and 399.1 eV (Fig. 1), respectively, and the missing of all the in-plane vibrational loss features (Fig. 4a). It is quite confusing that, at the first sight, for the low-exposure low-temperature state its N 1s binding energy is virtually identical to that of the N-bonded pyrrolyl while its C 1s binding energy is almost the same as the physisorbed pyrrole. Provided that the electronic/geometrical structure of the chemisorbed species does not deviate appreciably from that of the physisorbed pyrrole, both the C 1s and N 1s peaks should appear at lower binding energies relative to those of the physisorbed pyrrole due to the relaxation effect. As there is no sign for the dissociative adsorption of pyrrole at low exposure and low temperature, the lowering of the electron density on the carbonaceous moiety relative to nitrogen can account for the XPS result. Because pyrrole is an electron-rich molecule with the lowest ionization potential (8.28 eV) as compared to furan and thiophene [26], donation of its electrons to the substrate is possible. In particular, the highest occupied molecular orbitals, $1a_2$ and $2b_1$, which would be most susceptible to electrophilic attack, are π-orbitals mainly associated with the carbon atoms. Thus, on one hand, the relaxation effect upon adsorption will shift C 1s to lower binding energy; while on the other hand, electron donation will shift C 1s peak to the opposite direction. The counteraction can lead to the apparently invariant C 1s binding energy for the low temperature low coverage species.

From the above argument, it is reasonable to suggest that pyrrole adsorption at low exposure and low temperature employs a parallel configuration in order to maximize its interaction with the silicon substrate. Such a bonding configuration can rationalize the screening of all the in-plane vibrational modes as shown in Fig. 4a if the dipole selection rule is held [52]. This interpretation is similar to pyrrole adsorbed on Cu(1 0 0) given by Sexton [30]. On Cu(1 0 0), when a pyrrole multilayer was annealed to 200 K, only the γ(NH) and

γ(CH) modes at 560 and 760 cm^{-1} of B_2 symmetry were active. Combined with TDS, the lack of the A_1 and B_1 modes in the monolayer at 200 K is then interpreted as a solid evidence for parallel orientation of the pyrrole ring with respect to the Cu(1 0 0) plane. The π-bonded configuration is further supported by the binding energy difference between N 1s and C 1s for the low-exposure low-temperature species (114.4 eV) which is identical with that of pyrrole π-bonded on iron oxide (114.3 eV) [47].

At 1.5 L pyrrole exposure at 120 K or a 2.0 L pyrrole-exposed surface at 120 K followed by annealing to 200 K, a new loss feature at $\sim$2951 cm^{-1} can be readily spotted, implying the softening of some C–H bonds. It is possible that when the surface is getting more and more crowded, some π-bonded pyrrole molecules can employ a less parallel configuration due to geometrical restriction. Inevitably, the homogeneous π-interaction with the substrate is perturbed under such configuration. Then the interaction between pyrrole and Si(1 0 0) may mainly localize on certain ring carbon atoms which are comparatively closer to the surface, leading to the ν(CH) loss peak at lower frequency. An alternative explanation may be the formation of the cycloadduct between pyrrole and Si(1 0 0)-2×1 surface dimer, resulting in sp^3-rehybridized carbons, similar to furan or thiophene on Si(1 0 0)-2×1. However, at the time being, due to the intrinsically weak loss features, an unambiguous discrimination between these two configurations seems to be difficult.

Following the relaxation/electron donation argument, the shift of the C 1s binding energy from 284.7 to 284.2 eV when the surface is annealed to 350 K can be readily explained by the lifting of the π-electron donation due to reorientation from the nearly parallel pyrrole species to the vertical N-bonded pyrrolyl species. Based on the above discussion, a schematic description of the bonding geometries for pyrrole on Si(1 0 0)-2×1 under different conditions can be summarized as shown in Scheme 1.

The resulting pyrrolyl species is very stable and it survives to as high as 700 K at which temperature the pyrrolyl-related features are attenuated but not lost. Thus pyrrole shows much higher stability than furan or thiophene on Si(1 0 0)-2×1. For furan, decomposition occurs at about 350 K [14]; while for thiophene it is at about 450 K [15]. The deviation in the thermal stability between pyrrole and furan or thiophene can be partly attributed to surface passivation by depleted hydrogen from N–H group, as hydrogen may block the active sites necessary for pyrrolyl dissociation and its desorption temperature from monohydride is as high as 795 K [53]. The surface vacancy is essential for furan or thiophene dissociation, as inferred by the simultaneous occurrence of desorption and dissociation. Moreover, semiempirical calculations reveal the existence of considerable strain within the 2,5-dihydrofuran or 2,5-dihydrothiophene-like intermediate: the Si–Si–C angle in the formed Si_2C_4 ring is about 15° lower than the ideal tetrahedral angle [14,15]. Pyrrole is fortunately exempted from such an effect due to the formation of the N-bonded pyrrolyl species on Si(1 0 0)-2×1, which is believed to be another important factor which leads to its high thermal stability.

5. Conclusions

(1) Adsorption of pyrrole on Si(1 0 0)-2×1 at 120 K leads to molecularly π-bonded monolayer and physisorbed multilayer. The former changes its orientation from nearly parallel to tilted with respect to the silicon surface when surface coverage increases.
(2) Upon thermal annealing to 350 K, the π-bonded species converts to vertical N-bonded pyrrolyl species with the depleted H bonded to surface silicon atom. The pyrrolyl assembly is highly thermally stable, which does not dissociate until 700 K.
(3) At 900 K, about 50% of carbon and nitrogen atoms of the saturated pyrroyl layer are retained on the surface in the form of silicon carbide and silicon nitride.

Acknowledgements

This work was supported by the National University of Singapore under grant no. RP3981644.

References

[1] J.T. Yates Jr., Science 279 (1998) 335.
[2] R.J. Hamers, S.K. Coulter, M.D. Ellsion, J.S. Hovis, D.F. Padowitz, M.P. Schwartz, C.M. Greenlief, J.N. Tussell Jr., Acc. Chem. Res. 33 (2000) 617.
[3] R.A. Wolkow, Ann. Rev. Phys. Rev. 50 (1999) 413.
[4] A.V. Teplyakov, M.J. Kong, S.F. Bent, J. Am. Chem. Soc. 119 (1997) 11100.
[5] Y. Taguchi, M. Fujisawa, T. Takaoka, T. Okada, M. Nishijima, J. Chem. Phys. 95 (1991) 6870.
[6] B. Borovsky, M. Kueger, E. Ganz, J. Vac. Sci. Technol. B 117 (1999) 7.
[7] S.K. Coulter, J.S. Hovis, M.D. Ellison, R.J. Hamers, J. Vac. Sci. Technol. A 18 (2000) 1965.
[8] M.P. Schwartz, M.D. Ellison, S.K. Coulter, R.J. Hamers, J. Am. Chem. Soc. 122 (2000) 8529.
[9] M.D. Ellison, R.J. Hamers, J. Phys. Chem. B 103 (1999) 6243.
[10] T. Eicher, S. Hahuptmann, The Chemistry of Heterocycles, Thieme, Stuttgart, 1995.
[11] A. Tsumura, L. Tossi, H.E. Katz, Science 268 (1995) 270.
[12] T. Skotheim (Ed.), Handbook of Conducting Polymer, Dekker, New York, 1986.
[13] P. Batz, D. Schmeisser, W. Gopel, Phys. Rev. B 43 (1991) 9178.
[14] M.H. Qiao, F. Tao, Y. Cao, Z.H. Li, W.L. Dai, J.F. Deng, G.Q. Xu, J. Chem. Phys. 114 (2001) 2766.
[15] M.H. Qiao, Y. Cao, F. Tao, Q. Liu, J.F. Deng, G.Q. Xu, J. Phys. Chem. B 104 (2000) 11211.
[16] R. Konecny, D.J. Doren, J. Am. Chem. Soc. 119 (1997) 11098.
[17] M.H. Qiao, Y. Cao, J.F. Deng, G.Q. Xu, Chem. Phys. Lett. 325 (2000) 512.
[18] X. Cao, S.K. Coulter, M.D. Ellison, H. Liu, J. Liu, R.J. Hamers, J. Phys. Chem. B 105 (2001) 3759.
[19] (a) K. Seino, W.G. Schmidt, J. Furthmuller, F. Bechstedt, Phys. Rev. B 66 (2002), art. no. 235323;
(b) H. Luo, M.C. Lin, Chem. Phys. Lett. 343 (2001) 219.
[20] Silicon Carbide Electronic Materials and Devices, MRS Bull. 22 (1997).
[21] Y.S. Park (Ed.), SiC Materials and Devices, in: R.K. Willardson, R. Weber (Eds.), Semiconductors and Semimetals, vol. 52, Academic Press, San Diego, 1998.
[22] W.J. Choyke, H. Matsunami, G. Pensl (Eds.), Fundamental Questions and Applications of SiC, in: Special Issue of Physica Status Solidi (Phys. Status Solidi A 162 (1997), Phys. Status Solidi B 202 (1997)).
[23] K. Komeya, M. Matsui, High temperature engineering ceramics, in: M. Swain (Ed.), Structure and Properties of Ceramics, in: R.W. CahnP. Haasen, E.J. Kramer (Eds.), Materials Science and Technology, vol. 11, VCH, New York, 1996.
[24] Handbook of X-ray Photoelectron Spectroscopy, Perkin-Elmer Corporation, 1992.
[25] A.A. Bakke, H.W. Chen, W.L. Jolly, J. Electron Spectrosc. Related Phenom. 20 (1980) 333.
[26] N. Kishimoto, H. Yamakado, K. Ohno, J. Phys. Chem. 100 (1996) 8024.
[27] R.J. Hamers, Ph. Avouris, F. Bozso, J. Vac. Sci. Technol. A 6 (1988) 508.
[28] H. Wagner, R. Butz, U. Backes, D. Bruchmann, Solid State Commun. 38 (1981) 1155.
[29] R.C. Lord, F.A. Miller, J. Chem. Phys. 10 (1942) 328.
[30] B.A. Sexton, Surf. Sci. 163 (1985) 99.
[31] J.L. Bischoff, F. Lutz, D. Bolmont, L. Kubler, Surf. Sci. 251 (1991) 170.
[32] Y. Bu, D.W. Shinn, M.C. Lin, Surf. Sci. 276 (1992) 184.
[33] L. Porte, J. Appl. Phys. 60 (1986) 635.
[34] T. Bitzer, T. Alkunshalie, N.V. Richardson, Surf. Sci. 368 (1996) 202.
[35] R.M. Rummel, C. Ziegler, Surf. Sci. 418 (1998) 303.
[36] Th. Kugler, U. Thibaut, M. Abraham, G. Folkers, W. Göpel, Surf. Sci. 260 (1992) 64.
[37] S. Tanaka, M. Onchi, M. Nishijima, Surf. Sci. 191 (1987) L756.
[38] Y. Taguchi, M. Fujisawa, T. Takaoka, T. Okada, M. Nishijima, J. Chem. Phys. 95 (1991) 6870.
[39] Y. Bu, L. Ma, M.C. Lin, J. Phys. Chem. 97 (1993) 7081.
[40] T.L. Gilchrist, Heterocyclic Chemistry, third ed., Addison Welsley Longman Limited, London, 1997, Chapter 2.
[41] R.M. Ormerod, C.J. Baddeley, C. Hardacre, R.M. Lambert, Surf. Sci. 360 (1996) 1.
[42] M.N. Piancastelli, M.K. Kelly, G. Margaritondo, D.J. Frankel, G.J. Lapeyre, Surf. Sci. 211/212 (1989) 1018.
[43] F.Q. Yan, M.H. Qiao, X.M. Wei, Q.P. Liu, J.F. Deng, G.Q. Xu, J. Chem. Phys. 111 (1999) 8068.
[44] B.C. Wiegand, C.M. Friend, Chem. Rev. 92 (1992) 491.
[45] G.R. Schoofs, J.B. Benziger, Surf. Sci. 192 (1987) 373.
[46] F.P. Netzer, E. Bertel, A. Goldmann, Surf. Sci. 199 (1988) 87.
[47] F.M. Pan, P.C. Stair, T.H. Fleisch, Surf. Sci. 177 (1986) 1.
[48] C.J. Baddeley, C. Hardacre, R.M. Ormerod, R.M. Lambert, Surf. Sci. 369 (1996) 1.
[49] G. Tourillon, S. Raaen, T.A. Skotheim, M. Sagurton, R. Garrett, G.P. Williams, Surf. Sci. 184 (1987) L345.
[50] D.A. Blank, S.W. North, Y.T. Lee, Chem. Phys. 187 (1994) 35.
[51] C. Barckholtz, T.A. Barckholtz, C.M. Hadad, J. Am. Chem. Soc. 121 (1999) 491.
[52] H. Ibach, D.L. Mills, Electron Energy Loss Spectroscopy and Surface Vibrations, Academic Press, New York, 1982.
[53] G. Hess, M. Russel, B. Gong, J.G. Ekerdt, J. Vac. Sci. Technol. A 15 (1997) 1129.